Terminal-Aware Multi-Connectivity Scheduler for Uplink Multi-Layer Non-Terrestrial Networks

Michael N. Dazhi, Hayder Al-Hraishawi, Bhavani Shankar and Symeon Chatzinotas
Interdisciplinary Centre for Security, Reliability and Trust (SnT), University of Luxembourg.
emails: {michael.dazhi, hayder.al-hraishawi, bhavani.shankar, symeon.chatzinotas}@uni.lu

Abstract—This paper introduces the concept of multi-connectivity (MC) to the multi-orbit non-terrestrial networks (NTNs), where user terminals can be served by more than one satellite to achieve higher peak throughput. MC is a technique initially introduced by the 3rd Generation Partnership Project (3GPP) for terrestrial communications in 4G and 5G, it has shown much gain in the terrestrial domain and this paper explores areas where this concept can benefit the satellite domain. MC can increase throughput, but this entails increased power consumption at user terminal for uplink transmissions. The energy efficiency of uplink communications can be improved by designing efficient scheduling schemes, and to this end, we developed a terminal aware multi-connectivity scheduling algorithm. This proposed algorithm uses the available radio resources and propagation information to intelligently define a dynamic resource allocation pattern, that optimally routes traffic so as to maximize uplink data rate while minimizing the energy consumption at the UT. The algorithm operates with the terminal differentiating multi-layer NTN resource scheduling architecture, which has a softwarized dispatcher at the network layer that classifies and differentiates the packets based on terminal type. The performance of the proposed algorithm was compared with round robin and joint carrier schedulers in terms of uplink data rate and energy efficiency. We also provide architectural design of implementable schedulers for multi-orbital satellite networks that can operate with different classes of terminals.

I. INTRODUCTION

Satellite communications industry is on the verge of a major transformation due to the paradigm shift brought about by several key technological advancements such as software-defined satellites, very high throughput satellites (VHTS), non-geostationary orbit (NGSO) systems, virtualization and service orchestration [1]. Specifically, the recent developments are primarily focusing on deploying reconfigurable satellite payloads in order to offer generic and software-based solutions as well as to provide high throughput transmissions [2]. In addition to the established satellite applications like aeronautical, maritime, mapping, weather forecasting, and broadcasting, the recent advances have unlocked the satellite potentials to convey and execute various innovative use cases and new services from space [3]. Accordingly, satellite traffic demand is currently growing rapidly for provisioning affordable, accessible, uninterrupted wireless connectivity especially to the underserved and unserved areas. However, satellite resources are still scarce and usually expensive particularly in terms of

the radio frequency (RF) spectrum [4]. Therefore, it is crucial to devise unconventional techniques to improve resource utilization while satisfying the high data rate and low latency requirements.

In this direction, an intriguing concept has been recently studied within the multi-beam satellite architectures, that is dual connectivity (DC), which allows users to be simultaneously served with different systems and/or frequency bands [5]. Before that, the DC feature has been considered by the 3rd Generation Partnership Project (3GPP) in Release 12 for adoption to the fifth-generation (5G) New Radio (NR) specifications owing to its capability of maximizing the spectrum utilization and avoiding the traffic overload [6]. Likewise, the 3GPP group has been lately codifying the use of satellites and aerial platforms to construct multi-layer non-terrestrial networks (NTNs) in order to provide space-based 5G communication services and support future wireless ecosystems [7]. Thus, it is essential to extend the concept of DC to multi-connectivity (MC) to adapt to the flexibility and scalability offered by the emerging NTN architectures and the integrated space-aerial-terrestrial networks [8], [9].

The MC techniques are envisioned as an indispensable technology to significantly enhance the offered system capacity and improve the spectral efficiency in the heterogeneous networks. An important foreseeable application of MC is the interworking among various communication standards and architectures through allowing a smoother transition, e.g., between fourth generation (4G) and 5G systems [10]. The MC solution achieves not only higher per-user data rate but also provides mobility robustness, and thus, it can improve the resilience of wireless communications [11]. Additionally, data traffic in NTNs is vastly diversified and randomly distributed in the serving areas, and coming from various users with different quality-of-service (QoS) requirements [12]. Thus, employing MC in NTNs would help satisfying the asymmetry and heterogeneity of the traffic demands. However, when MC user terminals utilize multiple aggregated carriers/systems that inevitably comes at the cost of higher power consumption [13]. Further, the energy efficiency in NTNs is one of the major challenges, especially for the uplink transmissions and for the battery-limited mobile terminals [14].

In the literature, some contributions have studied and evaluated the issue of energy efficiency for the uplink transmissions
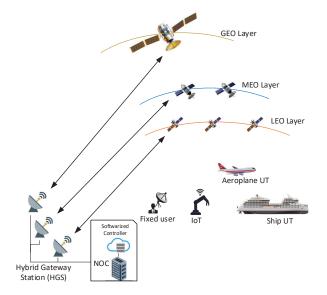
Fig. 1. Schematic diagram of the considered network topology of the Multi-layer NTN.

in satellite domain. For instance, the energy resource allocation problem in the uplink communications is investigated in [15] within the space-air-ground Internet of remote things networks, which aims at maximizing the system energy efficiency by jointly optimizing sub-channel selection and uplink transmission power control. In [16], a joint optimization model of spectrum efficiency and energy efficiency in a single-station multi-satellite MIMO system has been proposed based on a knee-point driven optimization algorithm. Further, a spatial group based optimal uplink power control scheme is proposed in [17] for enhancing the performance of random access in satellite networks. Additionally, two optimal power control schemes are proposed in [18] for maximizing both delay-limited capacity and outage capacity in cognitive satellite terrestrial networks, which are useful performance indicators for real-time applications. It is worth noting that the aforementioned works [15]–[18] do not consider concurrent aggregating multi-orbit scenarios in optimizing the uplink transmit power for satellite users.

Nevertheless, the MC promising performance enhancements in throughput and latency have motivated this work to further investigate the uplink energy efficiency issue from a user terminal standpoint. To the best of our knowledge, enhancement of the uplink transmit power has not been studied yet in the open literature within MC enabled multi-orbit NTNs.

Contributions: Our key technical contributions can be explicitly summarized as follows:

1) The design guidelines are outlined for the deployment of a multi-layer satellite network comprising of GEO, MEO and LEO satellites, which are all served by a multi-

orbital hybrid gateway station (HGS) [5]. This gateway station functions with a softwarized controller at the network layer, which performs functions including the classification and dispatching of PDUs onto different queues based on the terminal type of the transmitting user.

2) A terminal aware multi-connectivity (TAMC) scheduling algorithm has been developed, it considers the some radio parameters such as carrier-to-noise ratio (C/N) and the energy-per-bit-to-noise ratio (E_b/N_o) of the three satellite links. These information are required so as to achieve a resource allocation ratio that will allow for optimal resource allocation involving power and spectrum leading to a high capacity transmission with energy efficiency in the uplink.

3) The terminal aware multi-connectivity scheduler was designed based on 3GPP specification along with link budget analysis. The proposed algorithm was implemented by simulations and then compared to other state-of-the-art algorithms in terms of throughput and energy efficiency.

The rest of the paper is structured as follows. In section II, the network model and architecture is discussed extensively along with the problem analysis. The following Section III, focuses on the resource scheduling algorithms. While the simulation setup and performance evaluation is covered in Section IV. Finally, the conclusion and future work are summarised in Section V.

II. NETWORK MODEL AND SYSTEM ARCHITECTURE

A. Description of Topology and Architecture

The system topology consists of the three constellation of LEO, MEO and GEO satellites; a HGS controls the communication to these satellites through multiple inter-connected antenna ports, as shown in Fig. 1. The corresponding satellites then configure beams which provide coverage to different types of UTs, comprising fixed terrestrial, maritime, aeronautical, land-mobile and IoT type of UTs. The HGS is configured with a softwarized controller operating at the network layer, which performs the classification and dispatch of protocol data units (PDUs) onto different queues based on the user terminal type. This action allows the scheduling algorithm work efficiently and with high flexibility in optimizing the network KPIs.

The architecture of the radio scheduler (R/S) involves a queuing system which admits PDUs of UTs, each following a Markovian arrival process with arrival rate λ. The HGS will allocate various resource blocks (RBs) on different component carriers (CCs) of the three orbital satellites of LEO, MEO and GEO for uplink transmission, so that the UT can transmit the PDUs on the CCs. Figs. 2 and 3 show the architectures of the various types of schedulers that are considered in this paper, details of which are deferred to Section III. The scheduling algorithm is executed in the R/S unit, and it implements
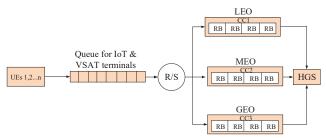
Fig. 2. Joint multi-layer NTN resource scheduling architecture where JC scheduler will run in R/S
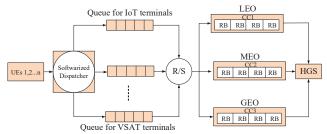

Fig. 3. Terminal differentiating multi-layer NTN resource scheduling architecture where TAMC or RR schedulers will run in R/S

the resource allocation process based on input radio link parameters including C/N and the E_b/N_o along with the information of the type of uplink UT. For this paper, the proposed uplink scheduling is achieved through the TAMC algorithm, and the types of terminals considered are the very small aperture terminal (VSAT) and internet of things (IoT) terminals as specified by 3GPP release 15 [7].

The conditions below have to be satisfied for the TAMC algorithm to perform the flexible resource allocation action.

- There must be sufficient E_b/N_o value to close the link budget for the LEO, MEO and GEO satellite links.
- The LEO, MEO and GEO satellites must have visibility at the HGS and at the considered UT. In addition, the UT should be capable of connecting to the three orbital constellations [19].
- The UT must be capable of providing the HGS with a unique terminal identifier, which will allow the softwarized dispatcher differentiate the UTs.

B. Uplink Transmission and Channel Model

The uplink transmission in a satellite network starts from the UT to the satellite in space through the radio channel, then down to the gateway station which connects to the network operation center (NOC) and the core network (CN). The satellite network is designed with a link budget and an air-interface that accounts for the power and gains required to achieve a successful transmission over a radio channel. The Free Space Loss (FSL) constitutes a significant reduction in power and takes the form,

$$FSL = 20\log(\frac{4\pi D}{\lambda}) \quad (1)$$

where λ is the wavelength of the radio frequency in meters and D is the propagation distance in meters. E_b/N_o is a figure of merit obtained at the receiver to ascertain the signal strength after transmission over a noisy channel and the impact of other contributing loss factors such as pointing and atmospheric losses. The radio air-interface is designed to be robust with sufficient E_b/N_o to mitigate losses in the satellite network, so as to achieve a low bit error rate (e.g. of the order of 10^{-6} and lower); this is done by employing advanced modulation and coding schemes. E_b/N_o is expressed in dB (2) [20] [21].

$$E_b/N_o = P_t + G_t + G_r - K - T_s - FSL - L_o - R \quad (2)$$

where P_t, G_t, G_r, L_o, T_s, K and R are transmit power, transmitter gain, receiver gain, other losses, receiver system noise temperature, Boltzmann constant and data rate in bits per second.

The E_b/N_o value can also be expressed as signal-to-noise ratio (SNR) normalised to spectral efficiency as shown in (3), where BW is bandwidth [21].

$$SNR = \frac{E_b}{N_o}\frac{R}{BW} \quad (3)$$

The radio channel is modelled as a Ricean distribution where the multipath fading has a dominant line of sight (LoS) along with some non-LoS components as indicated in [22], and (4) represents the probability density function of the Rician channel, with k being the $K-$factor of Rician distribution depicting the power ratio of the LoS and non-LoS components, Z being the signal power and I_0 denoting the Bessel function of the zeroth order.

$$P_{Rician}(Z) = k.e^{[-k(Z+1)]}I_0(2k\sqrt{Z}) \quad (4)$$

C. The Queuing Model

This system can be modelled as a $M/M/c$-PS queue with processor sharing (PS), where the first M represents the Markovian Poisson arrival and the second M stands for exponentially distributed service time, having c servers [23]. The UTs transmits the PDUs, which arrive the radio access network in a Markovian arrival process with arrival rate of λ, and the service time for PDU processing at the server is represented as μ. Hence the load of the system is given as $\rho = \frac{\lambda}{c.\mu}$ [24].

D. User Terminal

Two classes of terminals are considered in this paper; the IoT and VSAT terminals which are specified by 3GPP with design parameters outlined in Tables I. The network model, permits for a multi-orbital terminal device, that allows for a single UT to be able to establish multiple connections with satellites of different orbits. Nonetheless, the model also accommodates the installation of multiple antennas at the UT or premises especially for the VSAT scenario, in order to track multi-orbital satellites.

Parameters	LEO (VSAT)	LEO (IoT)	MEO (VSAT)	MEO (IoT)	GEO (VSAT)	GEO (IoT)
Satellite Altitude (Km)	1,500	1,500	10,000	10,000	35,786	35,786
Satellite G/T (dB/K)	13	1.1	20**	10**	28	19
UL Carrier Frequency (GHz)	30	2	30	2	30	2
Terminal speed (Km/hr)	upto 1,000km/hr	upto 1,000km/hr	upto 1,000km/hr	upto 1,000km/hr	upto 1,000km/hr	upto 1,000km/hr
One way propagation delay (ms)	25.83	25.83	95.19	95.19	272.37	272.37
UT Tx Gain (dBi)	43.2	8**	43.2	8**	43.2	8**
UT Transmit power (W)	2	6.2**	2	6.2**	2	6.2**
UT Transmit power (dBW)	3.01*	7.92*	3.01*	7.92*	3.01*	7.92*
Free Space Loss (dB)	185.51*	161.99*	201.99*	178.47*	213.06*	189.54*
Uplink C/N (dB)	23.31*	4.64*	13.82*	-2.94*	10.75*	-5.01*
Available EbNo (dB)	27.28*	8.64*	17.8*	1.04*	14.73*	-1.03*
* Derived **Assumed values						

E. Problem Analysis

The capacity enhancement is a non-convex linear optimization problem and a solution lies in the aggregation of the capacity (C) of the CCs of the LEO, MEO and GEO satellites, a technique known as MC.

$$C = BW \log_2(1 + SNR) \tag{5}$$

The average data rate can be expressed as

$$R = J.C \tag{6}$$

where J is the number of CCs.

In addition, the maximization of energy efficiency in the uplink for the UTs is also an important metric. The energy efficiency in bits-per-Joules (b/J) is given in (7) [26].

$$E = \frac{R}{P(R)} \tag{7}$$

where $P(R)$ is the transmission power needed to achieve a data rate of R.

III. RESOURCE SCHEDULING SCHEMES

This section discusses the three schedulers used in the paper namely the joint carrier (JC), round robin (RR) and the TAMC schedulers. For the ease of presentation, one satellite is assumed per constellation.

A. Joint Carrier Scheduler

The joint carrier (JC) scheduler in [26] operates with the scheduling architecture illustrated in Fig. 2. PDUs for both IoT and VSAT terminals arrive at a single queue to the R/S unit successively, where the first PDU (irrespective of the terminal type) is allocated to the RB of the CCs of appropriate satellites on the three orbits simultaneously. Subsequently, the next PDU of another UT on queue is scheduled also on the RB of all three orbital satellite CCs at once.

B. Round Robin Allocation Scheduler

The round robin (RR) scheduler operates with the scheduling architecture illustrated in Fig. 3. The architecture operates first by implementing the classification and differentiation of PDUs based on terminal type at the softwarized dispatcher. The dispatcher accepts the PDUs as input along with the identity (ID) of the transmitting UT, either IoT or VSAT. It then classifies the PDUs as IoT or VSAT, and then dispatch them in different queues based on their transmitting terminal IDs. At the R/S, the RR scheduler functions by allocating three different PDUs of the IoT and VSAT terminals successively, on the RB of each of the CCs of the three orbital satellites using the RR mechanism in [5].

$$\alpha'_{TL} = \frac{\frac{C/N_{TL}}{C/N_{TL}+C/N_{TM}+C/N_{TG}}}{\left(\frac{C/N_{TL}}{C/N_{TL}+C/N_{TM}+C/N_{TG}}\right) + \left(\frac{C/N_{VL}}{C/N_{VL}+C/N_{VM}+C/N_{VG}}\right)} \tag{8}$$

$$\alpha'_{VL} = \frac{\frac{C/N_{VL}}{C/N_{VL}+C/N_{VM}+C/N_{VG}}}{\left(\frac{C/N_{VL}}{C/N_{VL}+C/N_{VM}+C/N_{VG}}\right) + \left(\frac{C/N_{TL}}{C/N_{TL}+C/N_{TM}+C/N_{TG}}\right)} \tag{9}$$

$$\alpha_{TL} = \frac{\alpha'_{TL}}{\alpha'_{TL} + \alpha'_{TM} + \alpha'_{TG} + \alpha'_{VL} + \alpha'_{VM} + \alpha'_{VG}} \tag{10}$$

$$\alpha_L = \{\alpha_{TL}, \alpha_{VL}\} \tag{11}$$

$$\alpha_M = \{\alpha_{TM}, \alpha_{VM}\} \tag{12}$$

$$\alpha_G = \{\alpha_{TG}, \alpha_{VG}\} \tag{13}$$

* It should be noted that $0 \leq \alpha_{ik} \leq 1$, where i represents the UT of IoT (T) or VSAT (V); k represents orbital satellite links of LEO (L), MEO (M) or GEO (G). The same notation applies to C/N_{ik}.

C. Terminal-Aware Multi-connectivity Scheduler

The TAMC scheduler functions with the scheduling architecture shown in Fig. 3. When the PDUs arrive the R/S unit on different queues for IoT and VSAT, they are scheduled using the TAMC scheduler shown in Algorithm 1. TAMC requires E_b/N_o values of the three orbital satellites LEO, MEO and GEO, including the C/N of terminals with serving

satellite links. The TAMC algorithm uses the C/N inputs to arrive at a proportionality factor α and it is derived in equations (8) to (13), with which the RBs and CCs of the serving orbital satellites are allocated for both IoT and VSAT terminals, in a heuristic way driven by maximizing uplink capacity as well as enhancing energy efficiency. Once the proportionality factors are obtained, the TAMC algorithm will store the resource allocation sequence in a vector w having the dimension of available resources i.e, CCs, RBs and satellites where an entry 1 indicates the allocation of that resource. Then it will check the E_b/N_o values of all the links for the different terminals with the serving satellites of LEO, MEO and GEO to ascertain these values are above the QoS threshold, so as to implement the multi-connectivity optimization. In the absence of a beneficial scenario, the TAMC algorithm will revert to DC or a single carrier mode on the favorable satellite link.

The considered approach to improving data rate and enhancing energy utilization can further be achieved by proportionality factors (α), with which the different satellite orbital CCs can be aggregated in a multi-connected transmission scenario. These weights are a function of the C/N of the respective transmitting VSAT or IoT terminals of the serving orbital satellite. In particular, α_{TL}, α_{TM}, α_{TG}, α_{VL}, α_{VM} and α_{VG} in equations (11) to (13) are weights for IoT on LEO carrier, IoT on MEO carrier, IoT on GEO carrier, VSAT on LEO carrier, VSAT on MEO carrier and VSAT on GEO carrier respectively. While C/N_{TL}, C/N_{TM}, C/N_{TG}, C/N_{VL}, C/N_{VM} and C/N_{VG} are the IoT C/N on LEO CC, IoT C/N on MEO CC, IoT C/N on GEO CC, VSAT C/N on LEO CC, VSAT C/N on MEO CC and VSAT C/N on GEO CC respectively. Furthermore, α_L, α_M and α_G represents weights of LEO, MEO and GEO carriers respectively as can be seen in (8) to (13). Accordingly, the scheduler aims at maximizing the below expression.

$$\sum_{i=1}^{I} (\alpha_{iL}R_{iL} + \alpha_{Mi}R_{iM} + \alpha_{iG}R_{iG}) \ \forall i \in I \qquad (14)$$

R_{ik} is the data rate of i UT for k orbital satellite links of LEO (L), MEO (M), GEO (G) and (14) is subject to:

$$\mathbb{C}1 : min(E_b/N_{oL}, E_b/N_{oM}, E_b/N_{oG}) > \eta \ \ \forall i \in I$$

$$\mathbb{C}2 : E_i \geq \alpha_i \phi_{max} \ \ \forall i \in I$$

where η is a E_b/N_o threshold value, and E_i is the energy efficiency of UT_i with ϕ_{max} as the maximum transmit power utilization. Further mathematical treatment of this optimization problem will be performed in the future.

IV. PERFORMANCE EVALUATION

A. Simulation Setup

The simulation was setup with a link budget analysis using parameters outlined in Table I. The value of C/N at 50 MHz from Fig. 4, is used in deriving α, and for ease of

---

Algorithm 1: Terminal-aware Multi-Connectivity

Input:
Eb/No_L = LEO Eb/No
Eb/No_M = MEO Eb/No
Eb/No_G = GEO Eb/No
C/N_{T_L} = IoT C/N on LEO
C/N_{T_M} = IoT C/N on MEO
C/N_{T_G} = IoT C/N on GEO
C/N_{V_L} = VSAT C/N on LEO
C/N_{V_M} = VSAT C/N on MEO
C/N_{V_G} = VSAT C/N on GEO
Q_{LT} = Length of IoT PDU queue
Q_{LV} = Length of VSAT PDU queue
$\sigma = Q_{LT} + Q_{LV}$
$\eta = E_b/N_o$ Threshold
$j = 1$

1 **Carrier allocation ratio**
2 *LEO Carrier == α_L from (11)*
3 *MEO Carrier == α_M from (12)*
4 *GEO Carrier == α_G from (13)*
5 *Computing the multi-carrier allocation Sequence as w*
6 $w = (\alpha_L, \alpha_M, \alpha_G)$
7 **Carrier Allocation Implementation**
8 **while** $j \leq \sigma$ **do**
9   **if** E_b/N_{oG} and E_b/N_{oM} and $E_b/N_{oL} > \eta$ **then**
10 | Implement MC with w
11   **else**
12   Switch to single carrier mode on any available carrier
13   **if** E_b/N_{oG} and $E_b/N_{oM} > \eta$ **then**
14 | Implement DC with IoT on MEO CC; VSAT on both GEO and MEO CC
15   **else**
16   Switch to single carrier mode on any available carrier
17   **if** E_b/N_{oG} and $E_b/N_{oL} > \eta$ **then**
18 | Implement DC with IoT on LEO CC; VSAT on both GEO and LEO CC
19   **else**
20   Switch to single carrier mode on any available carrier
21   **if** E_b/N_{oM} and $E_b/N_{oL} > \eta$ **then**
22 | Implement DC with IoT and VSAT on both MEO and GEO CCs
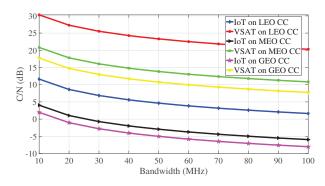23   **else**
24   Switch to single carrier mode on any available carrier
25 **end**

presentation, the same frequency band is used across all orbital layers. MATLAB was used to simulate the performance of the proposed algorithm while comparing other state-of-the-art algorithms.

B. Performance Analysis

The objective is to enhance the uplink capacity by implementing multi-connectivity, whilst reducing the energy utilization for the two classes of terminals using the TAMC scheduler. To optimize the uplink capacity along with energy efficiency in a heuristic way, the TAMC algorithm defines α using (8) to (13), such that $(\alpha_{TL}, \alpha_{VL}, \alpha_{TM}, \alpha_{VM}, \alpha_{VG}, \alpha_{TG})$ = (0.17, 0.17, 0.20, 0.13, 0.33, 0); α_{TG} is made 0 because of the low E_b/N_o value of -1.03 dB which cannot close the link, hence IoT terminals will not be scheduled on GEO CC by this scheduling algorithm. The RR will schedule IoT on MEO CC, VSAT on LEO CC and IoT on GEO CC per time with evenly divided weight values across the three available CCs, due to its operation limitation. Likewise JC is assumed to schedule only IoT since its PDU is first on the single queue, and this limitation is based on the architecture that it operates on, which only allows the first PDU on queue, of one particular type of terminal to be scheduled per time.

In Fig. 5, the data rate of the TAMC scheduler is compared to RR and JC schedulers, the data rate is plotted against traffic load ρ. The capacity C is derived from (5) with BW of 50 MHz set for each of the three CCs. The value of C varies from IoT and VSAT, depending on the particularly serving satellite, and this is because the value of E_b/N_o varies as shown in Table I. The plot shows that TAMC acheived average data rate of 138.45 Mbps, while RR and JC performed at 56.72 Mbps and 81.83 Mbps respectively when ρ is 0.1 load; it shows that TAMC out performs RR and JC by 83.75 % and 51.40 % respectively. The same percentage difference is noticed when ρ is at 0.5.

The performance of delay is shown in Fig. 6, which indicates same overlapping trend for TAMC, RR and JC schedulers. This is due to the usage of the three orbital layers by the three schedulers of TAMC, RR and JC. In Fig. 7, the energy efficiency in b/J is plotted against traffic load (ρ), and it shows the performance of TAMC compared with RR and JC. When ρ traffic load is 0.1, TAMC attains energy efficiency of 0.91 b/J, while RR and JC perform at 0.36 b/J and 0.48 b/J respectively. This shows that TAMC out performs RR and JC by 86.61 % and 61.87 % respectively. Even when ρ is 0.5, TAMC still out performs RR and JC by 85.71 % and 59.74 % respectively. During the scheduling process it was discovered that RR and JC experience limitation on the number of terminals and variety of satellite CCs they can utilize at once, thereby limiting their data rate and energy efficiency performance. TAMC is robust without limitations, as it can schedule all terminals including IoT and VSAT at the same time, utilizing all the available CCs of LEO, MEO and GEO satellites, in an intelligent resource allocation optimal
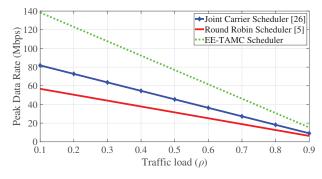

Fig. 4. C/N verses Bandwidth.
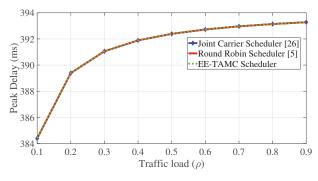

Fig. 5. Data rate verses traffic load.

Fig. 6. Delay verses traffic load.

pattern where data rate and energy efficiency are optimized with efficient utilization of the spectrum and system. This confirms TAMC is more superior to RR and JC.

V. CONCLUSIONS

In this paper, the uplink capacity and energy utilization of a satellite network is optimized by employing MC technique which aggregates the capacity of LEO, MEO and GEO CCs. A network topology was design of a multi-layer NTN with a HGS that connects to the three orbital satellites of LEO, MEO and GEO, allowing for the usage of MC at higher layers for the optimization of network performance aided by softwarized network controller and scheduling algorithms. A
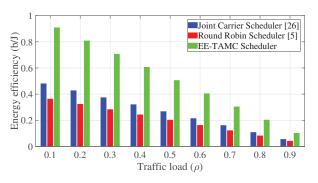
Fig. 7. Energy efficiency verses traffic load.

new scheduling architecture was also presented known as terminal differentiating multi-layer NTN resource scheduling architecture, that employs a softwarize dispatcher at the network layer which implements the terminal packet classification and dispatching. The dispatcher separates the PDUs onto different queues based on UT type of VSAT and IoT UTs. This architecture employs the proposed algorithm known as the TAMC algorithm, which intelligently defines the resource allocation pattern in form of a proportionality ratio α, that is derived based on C/N of the respective serving links to the various VSAT and IoT terminals. From the evaluation of the energy efficiency and throughput, TAMC outperformed RR and JC, confirming that TAMC is a superior uplink energy efficient scheduler with high capacity capabilities.

Future research areas that can be considered is the extension of this work to include many satellites in each of the three orbital layers; exploiting artificial intelligence and machine learning in the functionality of a robust optimizing scheduler.

REFERENCES

[1] L. Bertaux, S. Medjiah, P. Berthou, S. Abdellatif, A. Hakiri, P. Gelard, F. Planchou, and M. Bruyere, "Software defined networking and virtualization for broadband satellite networks," *IEEE Commun. Mag.*, vol. 53, no. 3, pp. 54–60, Mar. 2015.

[2] H. Al-Hraishawi, H. Chougrani, S. Kisseleff, E. Lagunas, and S. Chatzinotas, "A survey on non-geostationary satellite systems: The communication perspective," *IEEE Commun. Surveys Tuts.*, 2022.

[3] H. Al-Hraishawi, M. Minardi, H. Chougrani, O. Kodheli, J. F. M. Montoya, and S. Chatzinotas, "Multi-layer space information networks: Access design and softwarization," *IEEE Access*, 2021.

[4] T. Colin, T. Delamotte, and A. Knopp, "Filter distortions in ultra high-throughput satellites: Models, parameters and multicarrier optimization," *IEEE Trans. Signal Process.*, vol. 70, pp. 292–306, 2022.

[5] M. N. Dazhi, H. Al-Hraishawi, M. R. B. Shankar, and S. Chatzinotas, "Uplink capacity optimization for high throughput satellites using sdn and multi-orbital dual connectivity," in *2022 IEEE International Conference on Communications Workshops (ICC Workshops)*, 2022, pp. 544–549.

[6] 3rd Generation Partnership Project (3GPP), "Study on small cell enhancements for E-UTRA and E-UTRAN: Higher layer aspects," Standard, Jan. 2014, tR 36.842.

[7] 3rd Generation Partnership Project (3GPP), "Technical specification group radio access network; study on new radio (NR) to support non-terrestrial networks (release 15)," Standard, Jun. 2019, TR 38.811.

[8] 3rd Generation Partnership Project (3GPP), "Evolved universal terrestrial radio access (E-UTRA) and NR; multi-connectivity; stage 2," Standard, 2019, TS 37.340.

[9] H. Cui, J. Zhang, Y. Geng, Z. Xiao, T. Sun, N. Zhang, J. Liu, Q. Wu, and X. Cao, "Space-air-ground integrated network (SAGIN) for 6G: Requirements, architecture and challenges," *China Commun.*, vol. 19, no. 2, pp. 90–108, 2022.

[10] V. F. Monteiro, D. A. Sousa, T. F. Maciel, F. R. P. Cavalcanti, C. F. e Silva, and E. B. Rodrigues, "Distributed rrm for 5g multi-rat multi-connectivity networks," *IEEE Syst. J.*, vol. 13, no. 1, pp. 192–203, 2018.

[11] R. P. Antonioli, J. Pettersson, and T. F. Maciel, "Split responsibility scheduler for multi-connectivity in 5G cellular networks," *IEEE Network*, vol. 34, no. 6, pp. 212–219, 2020.

[12] H. Al-Hraishawi, E. Lagunas, and S. Chatzinotas, "Traffic simulator for multibeam satellite communication systems," in *10th Advanced Satellite Multimedia Syst. Conf. and the 16th Signal Process. for Space Commun. Workshop (ASMS/SPSC)*, 2020, pp. 1–8.

[13] H. Al-Hraishawi, N. Maturo, E. Lagunas, and S. Chatzinotas, "Scheduling design and performance analysis of carrier aggregation in satellite communication systems," *IEEE Trans. Veh. Technol.*, pp. 1–14, 2021.

[14] A. Mahbas, H. Zhu, and J. Wang, "Trio-connectivity for efficient uplink performance in future mobile hetnets," *IEEE Trans. Veh. Technol.*, vol. 69, no. 12, pp. 15 706–15 719, 2020.

[15] Z. Li, Y. Wang, M. Liu, R. Sun, Y. Chen, J. Yuan, and J. Li, "Energy efficient resource allocation for uav-assisted space-air-ground internet of remote things networks," *IEEE Access*, vol. 7, pp. 145 348–145 362, 2019.

[16] J. Zhang, B. Yu, C. Tang, Y. Zhang, L. Zhang, and S. Lu, "Joint optimization of energy efficiency and spectrum efficiency of single-station multi-satellite MIMO uplink system," in *IEEE Int. Conf. on Signal Processing, Commun. and Comput. (ICSPCC)*, 2021, pp. 1–6.

[17] B. Zhao, G. Ren, X. Dong, and H. Zhang, "Spatial group based optimal uplink power control for random access in satellite networks," *IEEE Trans. Veh. Technol.*, vol. 69, no. 7, pp. 7354–7365, 2020.

[18] S. Shi, G. Li, K. An, Z. Li, and G. Zheng, "Optimal power control for real-time applications in cognitive satellite terrestrial networks," *IEEE Commun. Lett.*, vol. 21, no. 8, pp. 1815–1818, 2017.

[19] ALL.SPACE, "All.space's first-of-its-kind terminal completes simultaneous, full performance, multi-link trials across all orbits — all.space." "https://all.space/insights/isotropic-systems-first-of-its-kind-terminal-completes-simultaneous-full-performance-multi-link-trials-across-all-orbits, 2022.

[20] A. Al-Saegh, A. Sali, J. Mandeep, A. Ismail, A. Al-Jumaily, and C. Gomes, *Atmospheric Propagation Model for Satellite Communications*. IntechOpen, 2014, ch. 09, p. 28.

[21] U. J. Lewark, J. Antes, J. Walheim, J. Timmermann, T. Zwick, and I. Kallfass, "Link budget analysis for future E-band gigabit satellite communication links (71-76 and 81-84 Ghz)," *CEAS Space Journal*, vol. 4, no. 1-4, pp. 41–46, 2013.

[22] Y. Lee and J. P. Choi, "Performance evaluation of high-frequency mobile satellite communications," *IEEE Access*, vol. 7, pp. 49 077–49 087, 2019.

[23] R. K. April, "Queueing Systems - Volume I : Theory," vol. I, pp. 1–21, 2015.

[24] V. Gupta, M. Harchol Balter, K. Sigman, and W. Whitt, "Analysis of join-the-shortest-queue routing for web server farms," *Performance Evaluation*, vol. 64, no. 9-12, pp. 1062–1081, 2007.

[25] 3rd Generation Partnership Project (3GPP), "Technical specification group radio access network; solutions for nr to support non-terrestrial networks (NTN) (release 16)," Standard, Jun. 2019, tR 38.821.

[26] F. Liu, K. Zheng, W. Xiang, and H. Zhao, "Design and performance analysis of an energy-efficient uplink carrier aggregation scheme," *IEEE J. Sel. Areas Commun.*, vol. 32, no. 2, pp. 197–207, 2014.